Real-time Validation of a DC-link Tuning Method for an AC-AC Wind Converter in Fractional Frequency Transmission System

Hamed Nademi, *Senior Member, IEEE*
Electrical and Computer Engineering Department
New Mexico State University
Las Cruces, NM 88003 USA

Kourosh Sedghisigarchi, *Senior Member, IEEE*
Electrical and Computer Engineering Department
California State University, Northridge
Northridge, CA 91330 USA

Luigi Vanfretti, *Senior Member, IEEE*
Electrical, Computer and Systems Engineering Department
Rensselaer Polytechnic Institute
Troy, NY 12180 USA

***Abstract*—Modularity and scalability features of matrix converters in wind farms paly pivotal role in interfacing the medium/high-power systems. These grids are vulnerable to instabilities during certain working conditions in addition to computational burden of existing control strategies, such as model predictive control (MPC). In this work, the operational performance of the Modular Multilevel Matrix Converter (M3C) is assessed to transmit power produced from offshore wind farm to interconnect with onshore AC grid. Small-signal impedance measurement-based stability analysis are not efficient to predict large-signal stability characteristics. The two-layer structure control design is proposed to regulate the converter branch voltages and currents. The second-layer iterative controller is embedded into an integrated perturbation analysis and sequential quadratic programming (IPA-SQP) method for handling uncertainty and overcome instability issues arise from capacitor voltage fluctuations. The complete control scheme objectives are lowering sampling time, optimization of variable constraints, and offering adaptive damping to enhance stability margin. The outcomes are verified via Real-Time simulation study using OPAL-RT platform for a designed 9-level M3C conversion system with an equal or low operating frequency at the input or output AC grids.**

Keywords—Converter, DC-link voltage, Predictive control, Stability, Wind power.

I. INTRODUCTION

The penetration pace of renewable energy sources into the medium- or high-voltage AC and DC systems, impose huge demands of design methodologies to adhere to the existing interfaces and new grid codes. With increased complexity, interfacing guidelines intend to be deteriorated to maintain the dynamic system performance at various operating scenarios. Interoperability and dynamic interactions are well understood to be a grand challenge for the large-scale integrated power grids. For the power conversion unit to interface among different power networks, it is important to offer scalability and modularity, direct AC-AC power conversion and high quality waveforms at the output terminal. Tremendous research studies have been conducted to utilize such conversion systems in high-torque/ low-speed AC drives, low-frequency AC transmission (LFAC) networks, and offshore wind energy [1]-[3]. Common application for deploying the M3C is LFAC transmission systems, taking advantage of lesser capacitive charging current through transmission line and better fault protection [3, 4]. The key control objectives in field applications using M3C technology are [1]-[3]: (a) energy balancing and flowing circulating currents inside the converter branches, (b) operational challenges with either equal frequency at input and output AC systems or very low output frequency (1 Hz to 20 Hz), (c) regulation of converter currents at the both input and output systems, and transferred power. Majority of different predictive-based solutions are within Model Predictive Control (MPC) category extensively adopted in multilevel power converters as addressed in [5]-[7]. FCS-MPC gives rather superior performance in real-time applications removing modulator and provides computational time reduction on embedded boards [6, 7]. There have been yet technical limitations to bridge the gaps on implementation of MPC solutions for the M3C [2, 8]. The available predictive strategies are heavily dependent on centralized control structures, restricting scalability feature of M3C along with the controller deficient in executing the calculations during control time interval. Distributed control concept has recently reported in [9] to improve controller performance. Most of the published solutions showing higher computational burden in real-time applications with large number of M3C cells incorporated. The phenomena of instantaneous fluctuations of cell capacitor voltages can lead to instability especially when variable speed generator is connected to the converter. Harmonic stability of high-voltage wind power system based on small-signal formulations is discussed in [10] with particular focus on the effects of passive filters to damp circulating currents inside modular multilevel converters.

Commonly used methods such as common-mode voltage injections [11] are suffering from cell voltage oscillations particularly if the generator is operated with fractional frequency. The proposed control strategy is formed to alleviate unbalanced voltages through circulating currents suppression. However, the challenge for control strategy is to tackle the induced common-mode voltage leading to offset DC in transferred branch powers when converter operates at critical frequencies; 0 Hz, 50/60Hz. As such, adaptive damping of capacitor voltage variations should be included in large part of control objectives. The research direction here is to minimize the required switching levels in the converter while preserving currents reference tracking in the input and output sides as well as regulation of branch voltages based on optimization predictive methodology. In recent years, an integrating of optimization algorithms are also recommended to meet the required sampling time for easy implementation on embedded boards [12]-[13], however, in such algorithms the sampling time does not provide less control efforts and improved performance. In this paper, a numerical optimization algorithm called an IPA-SQP framework is expanded to tackle the common challenges related to MPC

XXX-X-XXXX-XXXX-X/XX/$XX.00 ©20XX IEEE

optimal control in nonlinear systems with mixed constraints on state variables and control input [14, 15]. For instance, lately in [15], the IPA-SQP formulation has been applied to direct MPC and suggested to be an effective alternative for complex systems with MMCs family conversions. The developed control scheme is applied to the high-power wind turbine generation system which is interconnected to the electrical grid via 9-level M3C configuration. Real-time simulation analysis of the proposed controller with respect to model uncertainty in cell capacitance values, AC voltage dip and equal operating frequency for both the connected AC systems is examined.

II. Two-Layer Predictive Control And M3C Circuit Configuration

A. M3C Circuit Description

Fig. 1 presents a circuit of a (2n+1)-level M3C topology that interconnected two three-phase AC systems. M3C consists of 9 branches interfacing terminals of input system (i=a, b, c) to the phases of output side (j=u, v, w). The average value of the cells capacitor voltages must be controlled with low variation and zero power mean value during steady-state operation [2]. All the capacitors will be charged up and their voltage level remain within the average value of $\sum_{i=1}^{n} v_{Capi} \Big/ n$ by the used control strategy. Here, we assume 4cells per branch, thus there are 36 cells in the entire power conversion unit. According to [2, 3] the current flowing through the converter branches, i_{branch} is described as:

$$i_{branch} = \frac{i_{si}}{3} + \frac{i_j}{3} + i_{cir} \tag{1}$$

where circulating current i_{cir}, relates to the capacitor voltage dynamics of each cell. By inserting inductor into branches, each branch functions as current-controlled source for suppressing the *di/dt* and the transient currents, appearing in branches in time instant of cells selection process [1].

The state-space equations including control input and state variables, i.e., i_{branch} and $V_c{}^h{}_{ij}$ are obtained using (2). V_{branch} is the total voltage level of the all cluster cells in the converter unit. However, in our proposed control method, in which incorporates the voltage differences between neutral points of the two AC networks interconnected by M3C, the suppression of zero sequence voltage/current is achieved.

$$\begin{aligned} v_{branch} &= u_{si} - (L_s + \frac{L_{arm}}{3})\frac{di_{si}}{dt} - R_s i_{si} - e_j \\ &-(L_l + \frac{L_{arm}}{3})\frac{di_j}{dt} - R_l i_j - L_{arm}\frac{di_{branch}}{dt} - u_{ONe} \\ \frac{dv_{C_{ij}}{}^h}{dt} &= \frac{1}{C} S_i^k i_{branch} \qquad i,h = 1,\ldots n \end{aligned} \tag{2}$$

In [11], the aforementioned voltage difference (3) is determined as common-mode voltage, but still treated as fixed coefficient unlike what is happening in practice. Additional contribution of this work related to tolerances induced capacitor voltage fluctuations and communication time-delay due to the calculation instances among controllers which are uncertainties in the optimization process. The later aspects have not been fully studied in the literature with focus on the current research scope of M3C.

$$|u_{ONe}| = \frac{1}{9} \sum_{\substack{i=a,b,c \\ j=u,v,w}} \sum_{\varepsilon=1}^{36} v_{\varepsilon ij} \tag{3}$$

B. Problem Formulation of the Designed Predictive Control

The problem formulation of the proposed predictive strategy is displayed in the block diagram in Fig. 2. The executed steps of the IPA-SQP solver including stability formulation is detailed in Fig. 3. The one-step prediction horizon for the necessary state variables can be derived from (4) and cost function J comprising stability constraints is computed from (5):

$$\begin{aligned} i_{branch}(k+1) &= i_{branch}(k) - \frac{T_s}{2\left(L_s + L_l + \frac{L_{arm}}{3} + T_s(R_s + R_l)\right)} \cdot \\ &\left[u_{si}(k) - e_j(k) - v_{branch}(k+1)\right] \\ v_{Cij}(k+1) &= v_{Cij}(k) + S_i(k) \cdot \frac{T_s}{2C}\left(i_{branch}(k) + i_{branch}(k+1)\right) \end{aligned} \tag{4}$$

$$\begin{aligned} J = \alpha_1 \cdot \left\| i_{branch}^{ref}(k+1) - i_{branch}(k+1) \right\|^2 \\ + \alpha_2 \cdot \sum_{i=1}^{n} \left\| v_{Cij}(k+1) - V_{Cap\_dc}^{ref} \right\|^2 + \underbrace{\left| \dot{V}_{Lyapunov} \right|}_{Stability} \end{aligned} \tag{5}$$

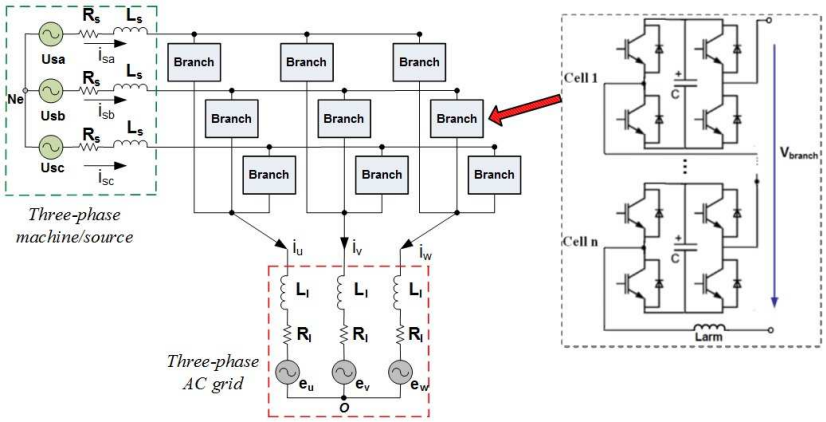

Fig. 1. Circuit diagram of a direct AC-AC M3C conversion interfaced via two different AC power systems.

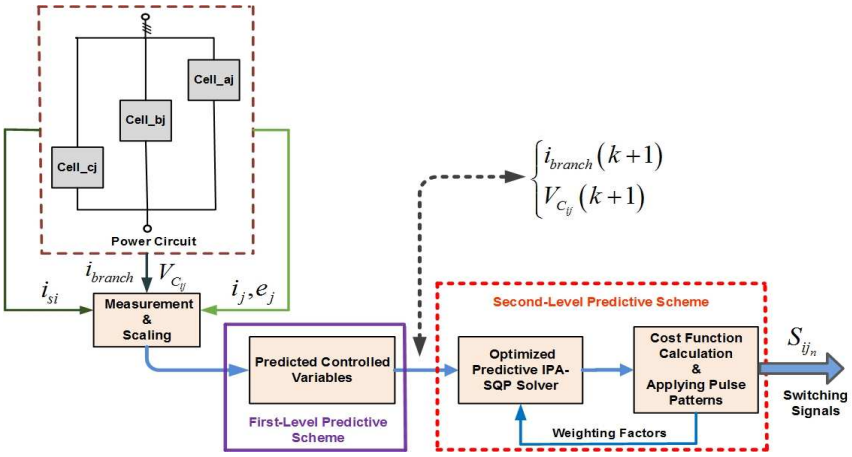

Fig. 2. Two-layer optimal predictive control structure generating the optimal switching pulses considering harmonics instability uncertainty.

To alleviate the issues due to parameters uncertainties, the constrained optimization of the system, as revealed in the flowchart Fig. 3 is refined in a way if at the point $x^i(t)+\delta x^i(t)$, where i is the iteration index, the Hamiltonian function (6) associated with the control state $u(t)$ is not small enough at prediction time instant k, thus the iterative procedure takes zero initial state perturbation $\delta x^i(t)=0$. More information and descriptions are given in [15, 16].

$$\sum_{k=t}^{t+N-1} \left\| H_u(k) \right\| \neq 0 \tag{6}$$

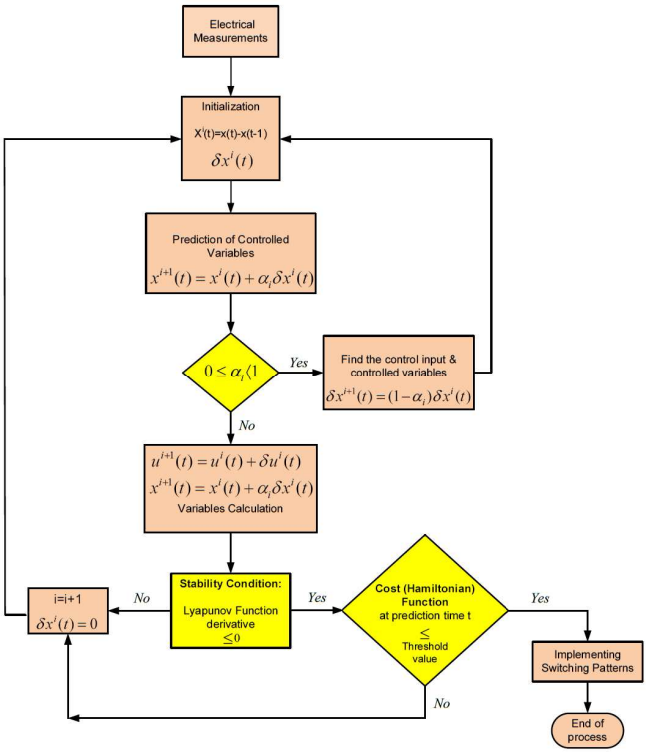

Fig. 3. Optimization strategy based on IPA-SQP applied within sampling period consisting predictive formulation and stability constraints.

III. Case Study Real-Time Simulation

The case-study evaluation is developed using RT Lab Software to be executed on OPAL-RT simulator via 9-level M3C for analyzing purposes concerning with the proposed controller and theoretical findings. Table I gives the main circuit parameters and specifications used in the analysis.

TABLE I. RATING PARAMETERS OF THE STUDIED SYSTEM WITH M3C

Parameters	Value	Parameters	Value
Full-bridge cell in each branch	4	Cluster capacitor voltage reference	1kV
Input frequency	2.5-50Hz	Output system resistor	6Ω
Input/ Output system voltage	6.6kV	Output system inductor	9mH
Input system resistor	1Ω	Sampling time	30μs
Input system inductor	3mH	Branch inductance	3mH
Output frequency	50Hz	Cell capacitance	3.3mF

Fig. 4 presents comparative results of the obtained capacitor voltage ripples as a function of different input AC system frequency. The theoretical fluctuations for capacitor voltages derived based on the method discussed in [11]. For this analysis, the output AC grid frequency is kept constant at 50Hz.

The measured ripples profile among capacitor voltages obtained by the proposed design denoting similar response within operation frequency band. An acceptable regulation over circulating current and common-mode voltage is achieved when converter interfaced with input/output AC systems using very low or similar operating frequency.

The ripples for higher frequency ranges demonstrate perfect match between measurements and theoretical findings. The capacitor voltages ripples effect in relation with damping ratio is shown in Fig. 5. A higher capacitance values offering poorer damping behavior, in which negatively impact on the converter stability operation. Despite majority of existing solutions, the developed control loop accounts the stability margin associated with cell capacitor voltage ripples through assessment of predicted poor damping mode. It is evident from Fig. 5 that cell capacitance value smaller than 5mF

achieved an acceptable damping behavior providing an optimal way of capacitor selection in design process.

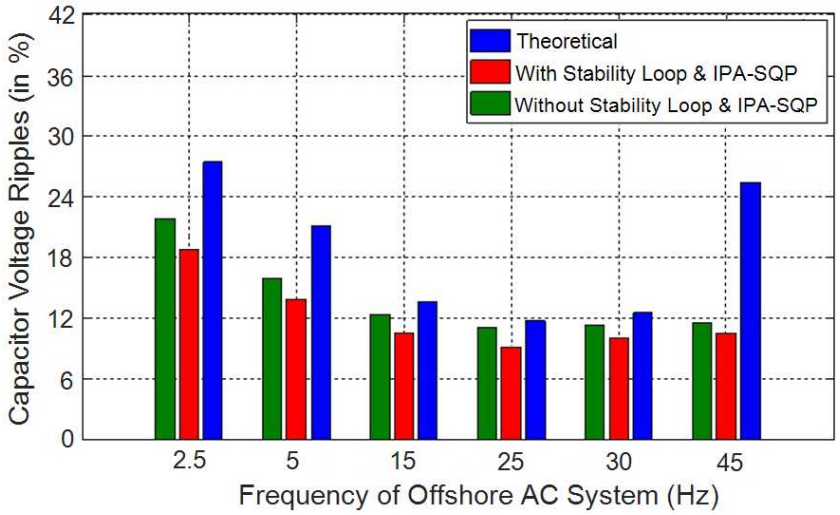

Fig. 4. Comparative results of capacitor voltage ripples at different input system frequency.

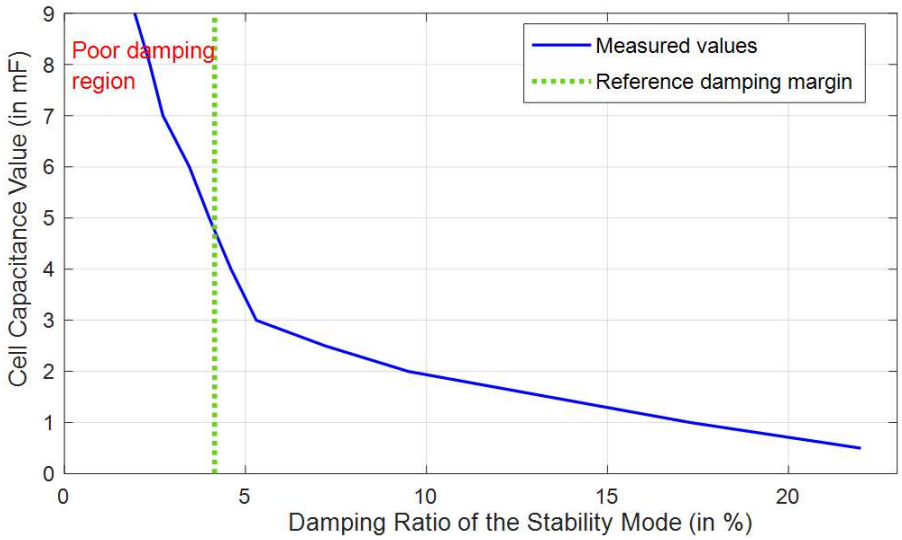

Fig. 5. Effects of cell capacitance value on the stability damping ratio due to the capacitor voltage fluctuations.

Real-time simulation performed to evaluate the dynamic response of the DC-bus made up of cluster of capacitor voltages when three-phase ground fault applied at input AC grid side. The fault happens at time instant t=0.5sec and it is cleared after 0.025sec. The obtained results are presented in Fig. 6 verifying the effectiveness of controller tuning process to damp the capacitor voltage variations smoothly so that the converter operates within stability region. As it can be seen from Fig. 6, without deploying DC-bus tuning method, capacitor voltages fluctuate as high as 25% compared to the reference voltage (1kV), while with the proposed control scheme capacitor voltages varying within 10% of the nominal voltage under fault condition.

The current distortion level also satisfies the common practice requirements specified by standards about harmonics performance. Fig. 7 shows the branch current 1 flowing through phase's au, and branch current 2 circulates between phase av, when the input/output AC system frequency is 50/25Hz. In this operating scenario the optimization algorithm is prioritized to suppress the high-frequency harmonics only in branch current 1. Obviously, in the branch current 2, high-frequency content is still presented.

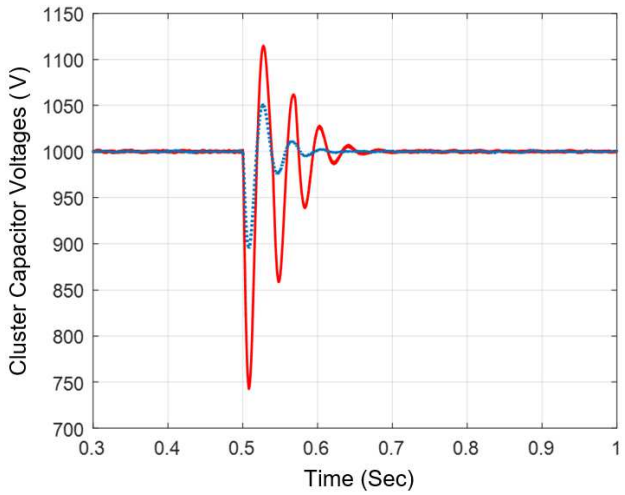

Fig. 6. Dynamic response of DC-bus capacitor voltages when ground fault occurs at t=0.5sec; Without (solid red line) and With (dotted blue line) activation of capacitor voltage tuning method.

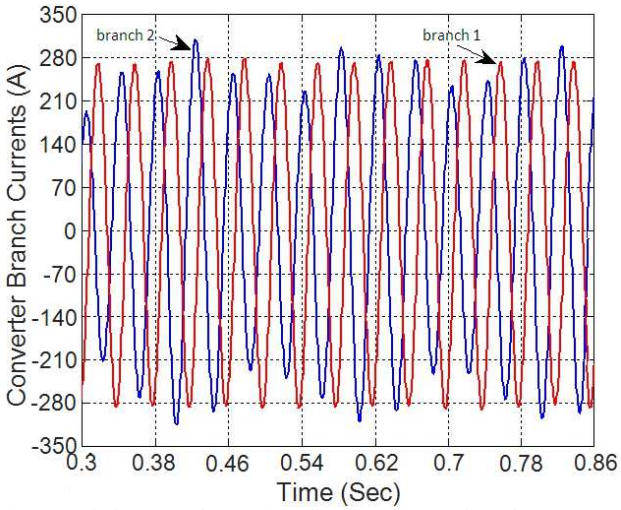

Fig. 7. High-frequency harmonics adjustment in M3C branch currents.

IV. Conclusion and Future Work

A satisfactory operation of the large-scale wind energy system depending on new modeling tools with particular focus on control developments to deal with the both transients and nonlinearities introduced from control loop interactions for system stability purposes. This paper has proposed an efficient two-level predictive control design for stable operation of a M3C converter interfaces wind farm to the interconnected onshore or utility grid operating at wide frequency range. This design includes an optimization effort in finding the cost function in each prediction horizon based on an integrated perturbation analysis and sequential quadratic programming (IPA-SQP) solution. The most critical barriers such as common-mode voltage, nonlinearities in conversion behavior, computational burden, and damping margin due to capacitor voltage tolerances are emphasized in the developed control strategy with real-time simulation analysis.

Effects of Transmission line interaction with the M3C converter and cable parameters on stability margin will be addressed in the future publication.

References

[1] C. Oates, "A methodology for developing 'chainlink' converters," in *Proc. of IEEE EPE* 2009, Sept. 2009, pp. 1-10.

[2] J. Luo, X.P. Zhang, *et al.*, "Harmonic Analysis of Modular Multilevel Matrix Converter for Fractional Frequency Transmission System," *IEEE Trans. Power Del.,* vol. 35, no. 3, pp. 1209-1219, June 2020.

[3] M. Diaz, R. Cardenas, *et al.*, "Control of Wind Energy Conversion Systems Based on the Modular Multilevel Matrix Converter," *IEEE Trans. Ind. Electron.,* vol. 64, no. 11, pp. 8799-8810, Nov. 2017.

[4] S. Liu, X. Wang, Y. Meng, *et al.*, "A Decoupled Control Strategy of Modular Multilevel Matrix Converter for Fractional Frequency Transmission System," *IEEE Trans. Power Del.,* vol. 32, no. 4, pp. 2111-2121, Aug. 2017.

[5] J. Rodriguez and P. Cortes, "Predictive Control of Power Converters and Electrical Drives," First Edition., *IEEE press-Wiley*, Mar. 2012.

[6] R. P. Aguilera, *et al.*, "Finite-Control-Set Model Predictive Control with Improved Steady-State Performance," *IEEE Trans. Ind. Informat.,* vol. 9, no. 2, pp. 658-667, May 2013.

[7] J. Rodriguez, M. P. Kazmierkowski, *et al.*, "State of the Art of Finite Control Set Model Predictive Control in Power Electronics," *IEEE Trans. Ind. Informat.,* vol. 9, no. 2, pp. 1003-1016, May 2013.

[8] A. Mora, M. Espinoza, *et al.*, "Model Predictive Control of Modular Multilevel Matrix Converter," in *Proc. of IEEE ISIE Conf.,*June 2015, pp. 1074-1079.

[9] S. Yang, Y. Tang, and P. Wang, "Distributed Control for a Modular Multilevel Converter," *IEEE Trans. Power Electron.,* vol. 33, no. 7, pp. 5578-5591, Jul. 2018.

[10] B. Zhang, and H. Nademi, "Modeling and Harmonic Stability of MMC-HVDC with Passive Circulating Current Filters," *IEEE Access.,* vol. 8, no. 7, pp. 129372-129386, Jul. 2020.

[11] B. Fan, K. Wang, P. Wheeler, *et al.*, "A Branch Current Reallocation Based Energy Balancing Strategy for the Modular Multilevel Matrix Converter Operating Around Equal Frequency," *IEEE Trans. Power Electron.,* vol. 33, no. 2, pp. 1105-1117, Feb. 2018.

[12] P. Karamanakos, T. Geyer, N. Oikonomou, *et al.*, "Direct Model Predictive Control: A Review of Strategies That Achieve Long Prediction Intervals for Power Electronics," *IEEE Ind. Electron. Magaz.,* vol. 8, no. 1, pp. 32-43, Mar. 2014.

[13] Z. Yan and J. Wang, "Model Predictive Control of Nonlinear Systems With Unmodeled Dynamics Based on Feedforward and Recurrent Neural Networks," *IEEE Trans. Ind. Informat.,* vol. 8, no. 4, pp. 746-756, Nov. 2012.

[14] Y. Xie, R. Ghaemi, "Model predictive control for a full bridge DC/DC converter," *IEEE Trans. Control Syst. Technol.*, vol. 20, no. 1, pp. 164-172, Jan. 2012.

[15] H. Nademi, R. Burgos, and Z. Soghomonian "Power Quality Characteristics of a Multilevel Current Source with Optimal Predictive Scheme from More-Electric-Aircraft Perspective," *IEEE Trans. Veh. Technol.*, vol. 67, no. 1, pp. 160-170, Jan. 2018.

[16] H. Park, and J. Sun, "A tutorial overview of IPA-SQP approach for optimization of constrained nonlinear systems," in *Proc. of* 11th *WCICA*, China, Jul. 2014, pp. 1735-1740.